Supporting Information

Establishing New Scaling Relations on Two-Dimensional MXenes for CO_2 Electroreduction

Albertus D. Handoko,[1,^] Khoong Hong Khoo,[2,^] Teck Leong Tan,[2] Hongmei Jin,[2,*] and Zhi Wei Seh[1,*]

[1]Institute of Materials Research and Engineering, Agency for Science, Technology and Research (A*STAR), 2 Fusionopolis Way, Innovis, Singapore 138634, Singapore

[2]Institute of High Performance Computing, Agency for Science, Technology and Research (A*STAR), 1 Fusionopolis Way, Connexis, Singapore 138632, Singapore

^These authors contributed equally to this work

*Corresponding authors: jinhm@ihpc.a-star.edu.sg (H.J.); sehzw@imre.a-star.edu.sg (Z.W.S.)

Supporting Information Section A: Preferred O-termination sites on M_2XO_2 MXenes

Prior to conducting adsorption studies, the most favourable O-termination site was determined by placing O atoms on both sides of bare M_2X MXene sheet and fully relaxing the structure. Table S1 list the preferred O-termination site on all MXenes examined in this study.

Table S1: Preferred O-termination site on M_2XO_2 MXenes

MXenes	Preferred O-termination site	
	FCC	HCP
Sc_2CO_2		✓
Ti_2CO_2	✓	
Zr_2CO_2	✓	
Hf_2CO_2	✓	
V_2CO_2	✓	
Nb_2CO_2	✓	
Ta_2CO_2	✓	
Cr_2CO_2		✓
Mo_2CO_2		✓
W_2CO_2		✓
Sc_2NO_2	✓	
Ti_2NO_2	✓	
Zr_2NO_2	✓	
Hf_2NO_2	✓	
V_2NO_2	✓	
Nb_2NO_2		✓
Ta_2NO_2		✓
Cr_2NO_2		✓
Mo_2NO_2		✓
W_2NO_2		✓

Supporting Information Section B: Atomic model of bare Ti_2C and O-terminated Ti_2CO_2 MXene

The atomic model of the most stable configuration of bare and O-terminated Ti_2C is presented in Figure S1. The alternative O termination position is also marked on Fig S1 (c). 19 Å of vacuum was added on the single layer O-terminated MXene to prevent the interaction of its periodic image (Fig S1 (d))

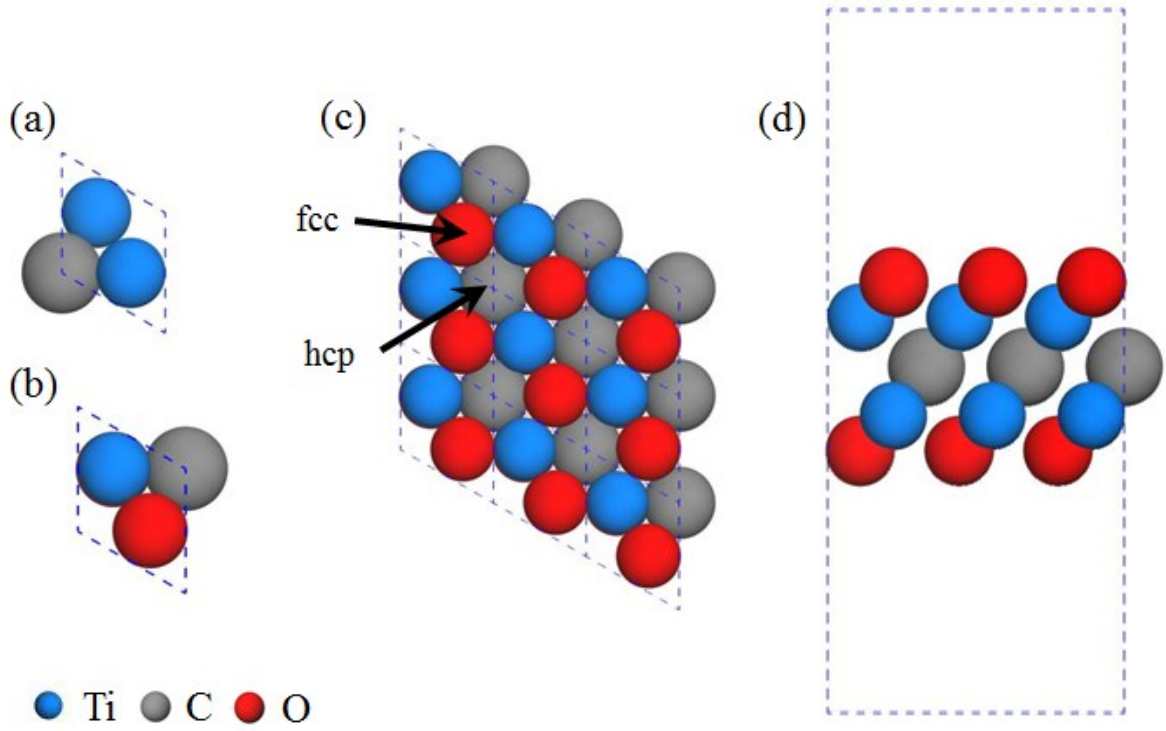

Figure S1: Atomic model of Ti_2CO_2 MXene: (a) (1×1) bare unit cell, (b) (1×1) O-terminated unit cell and the corresponding (3×3) O-terminated supercell as seen from the (c) top and (d) side. The alternative hcp hollow site favourable for O-termination on other M_2XO_2 MXenes is also marked in (c).

Supporting Information Section C: Methods

All density functional theory (DFT) calculations were performed using the Vienna Ab-initio Simulation Package (VASP),[1] and atomic potentials were treated using the projector augmented wave (PAW) method.[2] The generalised gradient approximation (GGA) in the Perdew-Burke-Ernzerhof form (PBE) was used for the exchange correlation functional and dispersion interactions were modelled within the DFT-D3 formalism.[3, 4] An energy cut-off of 450 eV defines the plane-wave basis set and structural relaxation was performed with a force component tolerance of 0.01 eV/Å. The Brillouin zones for our calculations were sampled using a Monkhorst-Pack grid of 8 × 8 × 1 and 2 × 2 × 1 *k*-points for the (1×1) and (3×3) supercells, respectively. The free energies for intermediates on the reaction pathway are calculated by adding the zero-point energy and entropy terms to the total energy. These corrections are calculated within the harmonic oscillator approximation where the degrees of freedom of adsorbates are treated as harmonic vibrations.[5] At least 18 Å layer of vacuum was added to prevent the interaction of its periodic image. Although we expect that practical CO_2RR will be performed on multi-layered MXenes, the single layer calculation performed here is justified as previous experimental and theoretical studies have shown that water and ionic species intercalation results in large (> 20 Å) *c*-lattice interlayer distance[6-8] – *i.e.* the layers are sufficiently separated to be treated as individuals.

The binding strength between the various intermediate adsorbates and different MXenes (ΔE_{ads}) were estimated using:

$$\Delta E_{ads} = E_{MXene+ads} - E_{MXene} - E_{ads}$$

Where $E_{MXene+ads}$ represents the energy of adsorbate modified MXene, E_{MXene} is the energy of MXene without adsorbate and E_{ads} is the energy of the adsorbate.

The relative Gibbs free energy of adsorbates can then be computed by:

$$\Delta G_{ads} = \Delta E_{ads} + \Delta E_{ZPE} - T\Delta S_{ads}$$

Where differential zero-point energy correction (ΔE_{ZPE}) and entropy correction ($T\Delta S_{ads}$) are taken into account.

Supporting Information Section D: Minimum energy pathway diagram for M_2XO_2 MXenes

In Figure S2 we show the minimum energy pathway diagrams for all 19 MXenes. Sc_2CO_2 was excluded from calculation because of significant substrate distortion and large fluctuations in the binding energy when intermediates are introduced. The reaction energy calculation for *CO is included on all substrates as a comparison with the *HCOOH pathway. A summary of the shortest adsorbate distance to the O-terminated surface is presented in Table S2.

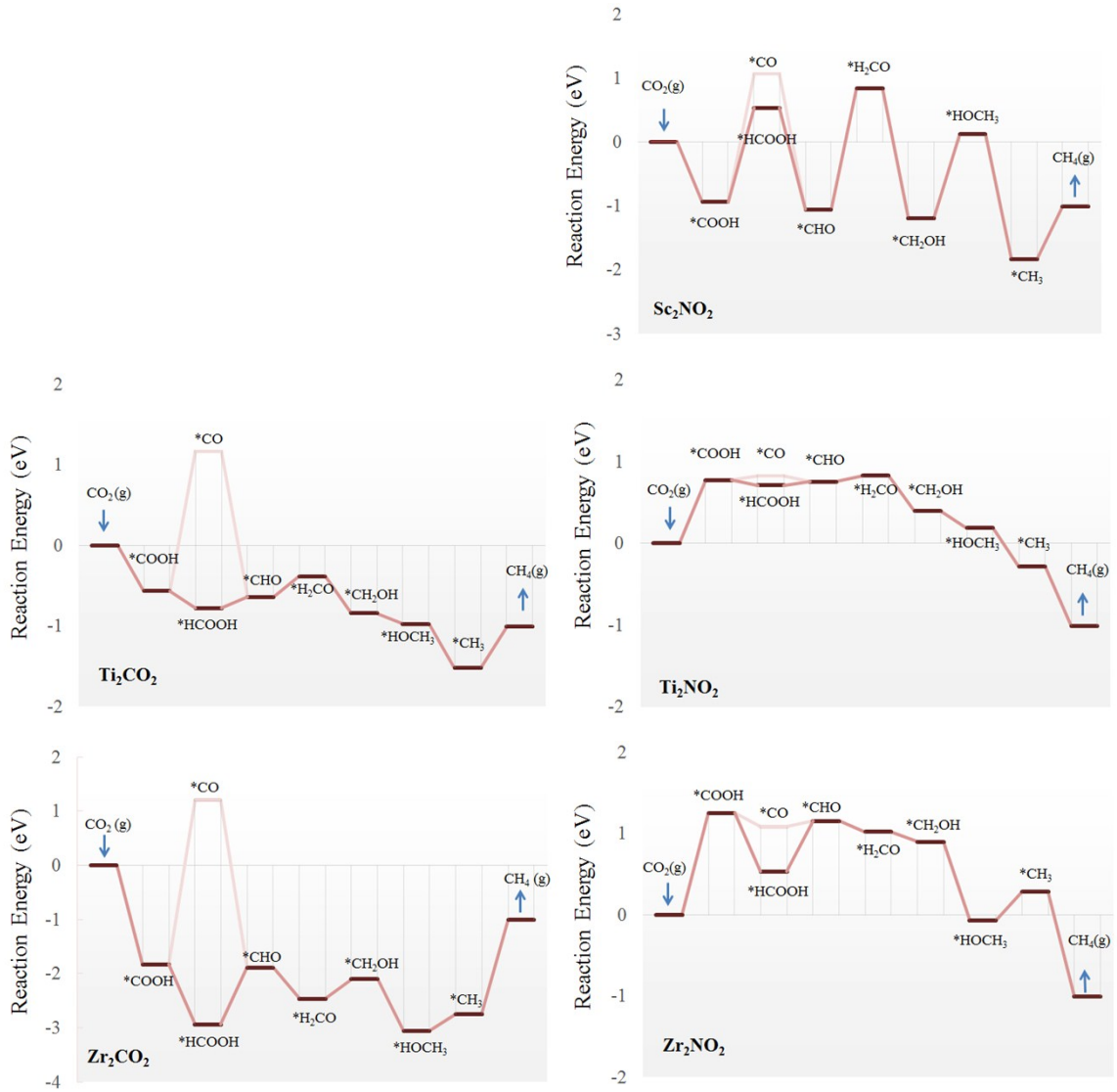

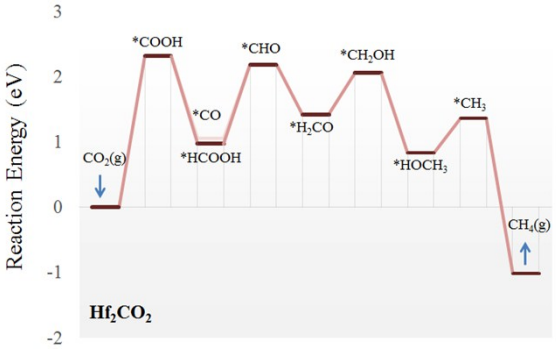
Reaction Energy (eV)
3
2
1
0
-1
-2
CO2(g)
*COOH
*CO
*HCOOH
*CHO
*H2CO
*CH2OH
*HOCH3
*CH3
CH4(g)
Hf2CO2

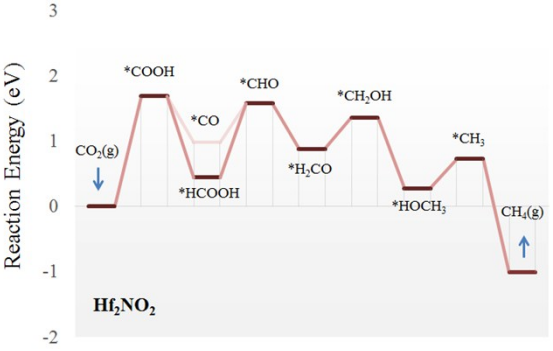
Reaction Energy (eV)
3
2
1
0
-1
-2
CO2(g)
*COOH
*CO
*HCOOH
*CHO
*H2CO
*CH2OH
*HOCH3
*CH3
CH4(g)
Hf2NO2

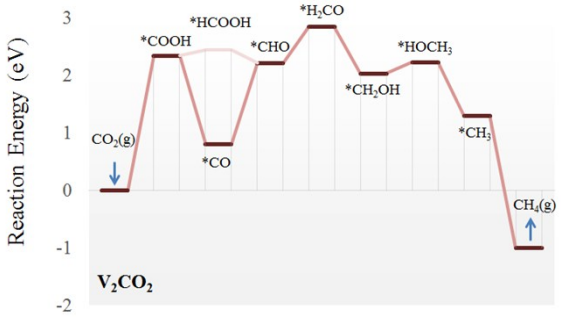
Reaction Energy (eV)
3
2
1
0
-1
-2
CO2(g)
*COOH
*HCOOH
*CO
*CHO
*H2CO
*HOCH3
*CH2OH
*CH3
CH4(g)
V2CO2

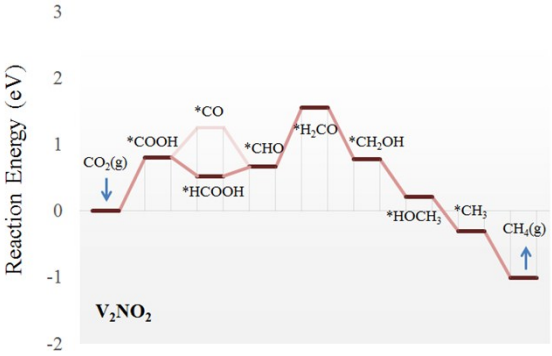
Reaction Energy (eV)
3
2
1
0
-1
-2
CO2(g)
*CO
*COOH
*HCOOH
*CHO
*H2CO
*CH2OH
*HOCH3
*CH3
CH4(g)
V2NO2

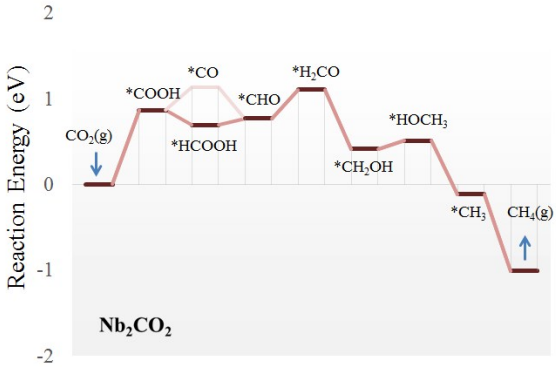
Reaction Energy (eV)
2
1
0
-1
-2
CO2(g)
*CO
*COOH
*HCOOH
*CHO
*H2CO
*HOCH3
*CH2OH
*CH3
CH4(g)
Nb2CO2

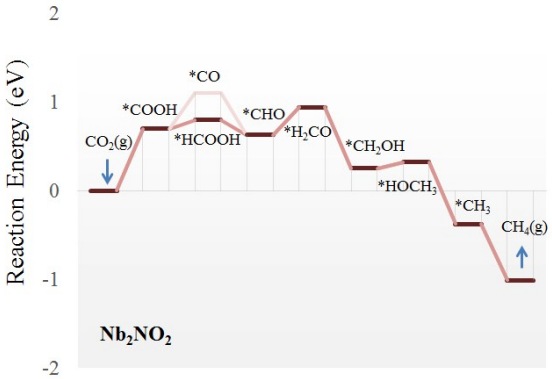
Reaction Energy (eV)
2
1
0
-1
-2
CO2(g)
*CO
*COOH
*HCOOH
*CHO
*H2CO
*CH2OH
*HOCH3
*CH3
CH4(g)
Nb2NO2

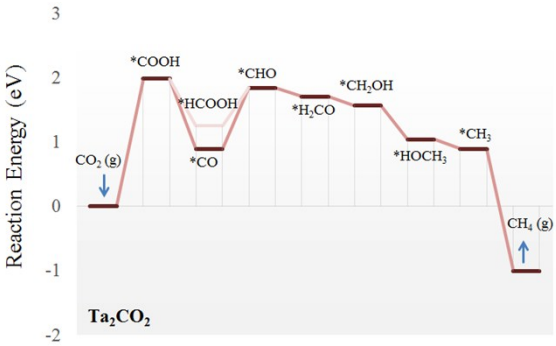
Reaction Energy (eV)
3
2
1
0
-1
-2
CO2 (g)
*COOH
*HCOOH
*CO
*CHO
*H2CO
*CH2OH
*HOCH3
*CH3
CH4 (g)
Ta2CO2

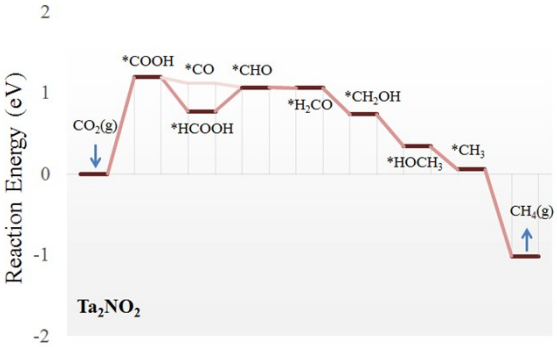
Reaction Energy (eV)
2
1
0
-1
-2
CO2(g)
*COOH
*CO
*HCOOH
*CHO
*H2CO
*CH2OH
*HOCH3
*CH3
CH4(g)
Ta2NO2

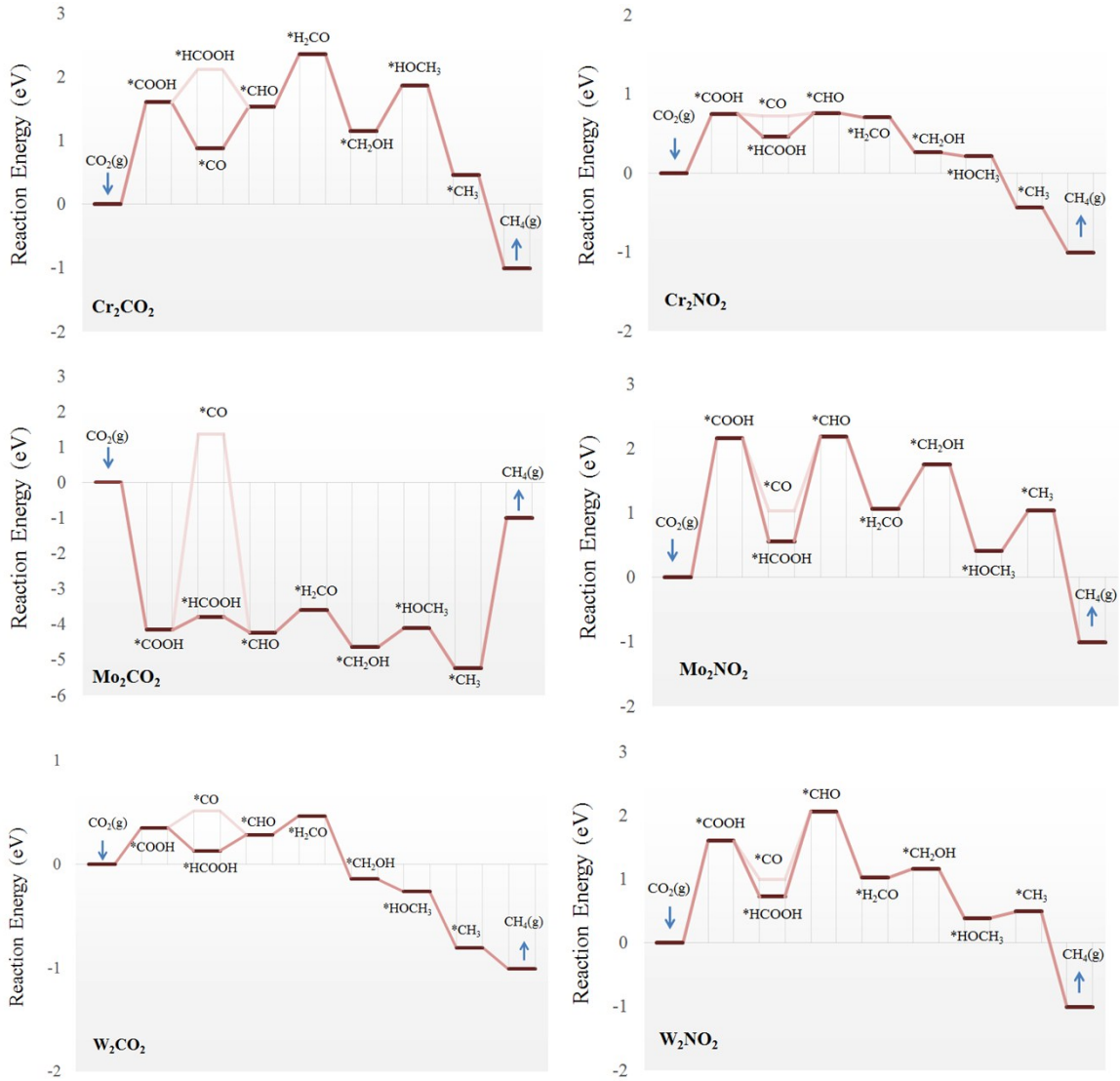

Figure S2: Minimum energy pathway diagrams for M_2XO_2 MXenes in this study.

Table S2: The adsorption configuration and list of the shortest distance (Å) between adsorbed intermediate and the M_2XO_2 MXene.

MXenes	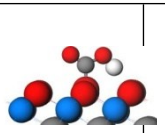 *COOH	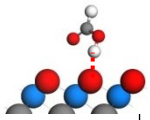 *HCOOH	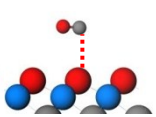 *CO	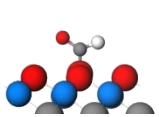 *CHO	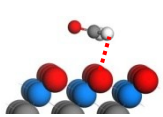 *H_2CO	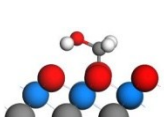 *CH_2OH	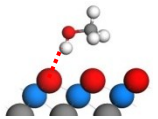 *$HOCH_3$	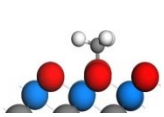 *CH_3
Ti_2CO_2	1.428	1.821	3.009	1.397	2.816	1.481	2.405	1.450
Zr_2CO_2	1.402	1.650	3.037	1.387	2.865	1.473	2.615	1.454
Hf_2CO_2	1.420	1.778	3.031	1.394	2.923	1.483	1.982	1.460
V_2CO_2	1.435	1.807	2.968	1.399	2.796	1.482	2.640	1.445
Nb_2CO_2	1.434	1.782	3.011	1.400	2.872	1.490	2.680	1.456
Ta_2CO_2	1.453	1.791	2.952	1.414	2.833	1.506	2.627	1.463
Cr_2CO_2	1.540	1.737	2.922	1.454	2.243	1.539	2.342	1.456
Mo_2CO_2	1.543	1.774	3.009	1.462	2.860	1.557	2.455	1.467
W_2CO_2	1.588	1.842	2.965	1.478	2.722	1.578	2.489	1.474

Sc_2NO_2	1.410	1.599	2.965	1.382	2.752	1.467	1.680	1.456
Ti_2NO_2	1.448	1.783	2.978	1.412	2.784	1.489	3.089	1.452
Zr_2NO_2	1.427	1.706	2.953	1.397	2.893	1.479	2.445	1.454
Hf_2NO_2	1.445	1.614	2.995	1.412	2.864	1.494	1.915	1.462
V_2NO_2	1.444	1.806	2.952	1.405	2.746	1.492	1.936	1.451
Nb_2NO_2	1.487	1.875	2.966	1.434	2.632	1.526	1.933	1.456
Ta_2NO_2	1.507	1.865	2.957	1.445	2.784	1.539	1.972	1.464
Cr_2NO_2	1.568	1.909	2.994	1.461	2.532	1.560	2.260	1.452
Mo_2NO_2	1.549	1.945	3.008	1.453	2.736	1.561	2.105	1.465
W_2NO_2	1.543	1.899	2.951	1.438	2.702	1.565	2.094	1.467

Supporting Information Section E. Activity and selectivity of M_2XO_2 MXenes towards CO_2RR

In Table S3 we list the theoretical limiting potential for CO_2RR ($U_L(CO_2)$) representing the CO_2RR activity,[9, 10] and $U_L(CO_2) - U_L(H_2)$ representing selectivity of CO_2RR with respect to HER.[11] the $U_L(H_2)$ values were obtained from previous computational work using a similar approach.[12]

Table S3: The activity and selectivity for all M_2XO_2 MXenes in this study, arranged in order of decreasing $U_L(CO_2)$ values.

MXene	$U_L(CO_2)$ (V vs. RHE)	$U_L(H_2)$ (V vs. RHE)	$U_L(CO_2) - U_L(H_2)$ (V)
W_2CO_2	-0.349	-0.572	0.223
Ti_2CO_2	-0.516	-0.358	-0.158
Nb_2NO_2	-0.699	-0.087	-0.612
Cr_2NO_2	-0.748	-0.379	-0.369
Ti_2NO_2	-0.771	-0.284	-0.487
V_2NO_2	-0.803	-0.067	-0.736
Nb_2CO_2	-0.865	-0.336	-0.529
Ta_2NO_2	-1.192	-0.512	-0.680
Zr_2NO_2	-1.248	-0.318	-0.930
W_2NO_2	-1.596	-1.034	-0.562
Cr_2CO_2	-1.602	-0.604	-0.998
Hf_2NO_2	-1.683	-0.045	-1.638
Zr_2CO_2	-1.735	-1.005	-0.730
Sc_2NO_2	-1.899	-1.356	-0.543
Ta_2CO_2	-1.982	-0.747	-1.235
Mo_2NO_2	-2.156	-1.093	-1.063
Hf_2CO_2	-2.310	-1.266	-1.044
V_2CO_2	-2.341	-0.211	-2.130
Mo_2CO_2	-4.227	-0.048	-4.179

References cited in the Supporting Information

1 G. Kresse and J. Furthmüller, *Phys. Rev. B*, 1996, **54**, 11169-11186.

2 G. Kresse and D. Joubert, *Phys. Rev. B*, 1999, **59**, 1758-1775.

3 J. P. Perdew, K. Burke and M. Ernzerhof, *Phys. Rev. Lett.*, 1996, **77**, 3865-3868.

4 S. Grimme, J. Antony, S. Ehrlich and H. Krieg, *J. Chem. Phys.*, 2010, **132**, 154104.

5 C. J. Cramer, *Essentials of Computational Chemistry: Theories and Models, 2nd Edition*, Wiley, Chichester, West Sussex, England, 2004.

6 Y. Xie, M. Naguib, V. N. Mochalin, M. W. Barsoum, Y. Gogotsi, X. Yu, K. W. Nam, X. Q. Yang, A. I. Kolesnikov and P. R. Kent, *J. Am. Chem. Soc.*, 2014, **136**, 6385-6394.

7 K. D. Fredrickson, B. Anasori, Z. W. Seh, Y. Gogotsi and A. Vojvodic, *J. Phys. Chem. C*, 2016, **120**, 28432-28440.

8 A. D. Handoko, K. D. Fredrickson, B. Anasori, K. W. Convey, L. R. Johnson, Y. Gogotsi, A. Vojvodic and Z. W. Seh, *ACS Appl. Energy Mater.*, 2017, **1**, 173-180.

9 K. Chan, C. Tsai, H. A. Hansen and J. K. Nørskov, *ChemCatChem*, 2014, **6**, 1899-1905.

10 A. A. Peterson, F. Abild-Pedersen, F. Studt, J. Rossmeisl and J. K. Norskov, *Energy Environ. Sci.*, 2010, **3**, 1311-1315.

11 X. Hong, K. Chan, C. Tsai and J. K. Nørskov, *ACS Catal.*, 2016, **6**, 4428-4437.

12 Z. W. Seh, K. D. Fredrickson, B. Anasori, J. Kibsgaard, A. L. Strickler, M. R. Lukatskaya, Y. Gogotsi, T. F. Jaramillo and A. Vojvodic, *ACS Energy Lett.*, 2016, **1**, 589-594.